Exploding-wire experiments and theory for metal conductivity evaluation in the sub-eV regime

J. Stephens and A. Neuber
Center for Pulsed Power and Power Electronics, Texas Tech University, Lubbock, Texas 79409, USA
(Received 28 September 2012; published 18 December 2012)

Copper and silver wires are subjected to pulsed high current densities producing high density metal plasma in the sub-eV regime with atmospheric air as a background gas. Numerical simulation via application of the one-dimensional magnetohydrodynamic partial differential equations solved simultaneously with the constraining circuit equations is presented. The simulations require accurate knowledge of the material equation of state (EOS) and transport properties; the LANL SESAME database is applied for the EOS in all cases. Two electrical conductivity models are applied. First, the Lee-More-Desjarlais (LMD) and its modification, the quantum LMD (QLMD) conductivity, which have been well proven at higher temperatures, are applied. Simulations with the LMD and QLMD data indicate that the conductivity data as well as the MHD methodology are accurate in the sub-eV regime of interest. A less computationally involved, empirical conductivity model is applied in the same regime to explore its temperature-density range of applicability compared to the more sophisticated model.

DOI: 10.1103/PhysRevE.86.066409 PACS number(s): 52.80.Qj, 52.27.Gr, 52.30.Cv, 52.50.Nr

I. INTRODUCTION

Current induced electrical explosions of conductors have become a common mechanism for both producing experimental electrical conductivity data [1–8] and verifying existing conductivity models [9–13] for strongly coupled metal plasma. Similar to the methodologies of Refs. [9–13], this paper compares voltage and current waveforms obtained from exploding-wire (EW) experiments, with magnetohydrodynamic (MHD) simulations, to assess the accuracy of the equation of state (EOS) and transport models applied within the MHD simulation.

In practice, EWs are widely used as high current opening switches [14–20] owing to the sharp decrease in conductivity experienced between vaporization and the critical point. Silver and copper are generally accepted as the optimum switching materials [19,20] and are the materials under investigation here. The experiments presented exhibit a specific emphasis on the sub-eV (<11.5 kK) switch type current interruption process, a region which has received little attention compared to its higher temperature counterpart.

It is a common practice to submerge the EW in a semi-incompressible media, such as water, for studies such as these. Under these conditions, the wire expansion is restricted, thus limiting hydroexpansive cooling of the plasma column and allowing for the production of extremely high temperatures (e.g., >90 kK in Ref. [11]). Since this study is primarily aimed at sub-eV temperatures, the desired parameter range is simply achieved in air at atmospheric pressure.

II. EXPERIMENTAL SETUP

The experimental setup given in Fig. 1 is used to drive the EWs described in these experiments. The capacitor shown in Fig. 1 is initially charged to a controlled voltage V_0. At a controlled time, the thyratron switch is closed. The switch used requires eight parallel, short (∼5 ns) RG213 coaxial transmission lines to uniformly distribute the current density inside of the thyratron. Upon closing of the switch, several kiloamps of current are passed through the EW, inducing dense metal plasma formation within a few microseconds. In each experiment, the exploding wire has a 127-μm diameter and 18-cm length.

The circuit shown in Fig. 1 is modeled as a series resistor inductor capacitor (RLC) circuit. Experimentally, a short circuit was compared with the numerical simulation to verify the accuracy of the circuit model.

Parasitic inductance in the experimental setup has to be considered when the resistive voltage drop across the EW is desired. As a result, the following equation is used to derive the resistive voltage drop across the EW from the charging voltage and pulsed current, with $C = 1.85$ μF and $L = 2.7$ μH.

$$V_R(t) = V_0 - \frac{1}{C}\int_0^t i(t')dt' - L\frac{di(t)}{dt}. \tag{1}$$

III. THEORETICAL MODEL

It is known that EWs demonstrate significant stratification along the axis of the wire [14,21–23]. Abramova *et al.* present that the time for MHD instability development can be approximated by $\tau_{\mathrm{MHD}} \approx 2(\rho/\mu_0)^{1/2}/j_{\max}$, which is on the order of 0.5–1 μs for the experiments discussed here [21]. In these studies, the wire explosion is a multiple-microsecond process; therefore, it is expected that the instabilities will have sufficient time to develop. However, the wires generally exhibit an approximate, or average, cylindrical behavior. Consequently, one-dimensional numerical methods have been widely applied with a high level of success [8–16,24–26]. Although alternatives to MHD have been successfully applied to model exploding conductors [14,27], MHD is the method of choice here.

The one-dimensional, radially directed MHD equations in Lagrangian coordinates are given as [28]

$$\frac{\partial \rho}{\partial t} + v\frac{\partial \rho}{\partial r} + \rho\frac{\partial v}{\partial r} + \frac{\rho v}{r} = 0, \tag{2a}$$

$$\rho\frac{\partial v}{\partial t} + \rho v\frac{\partial v}{\partial r} = -j_z B_\varphi - \frac{\partial p}{\partial r}, \tag{2b}$$

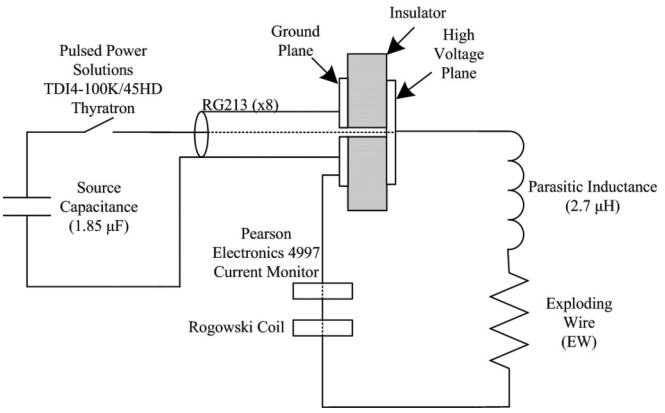

FIG. 1. Exploding-wire experimental setup.

$$\rho\frac{\partial u}{\partial t}+\rho v\frac{\partial u}{\partial r}=-p\frac{\partial v}{\partial r}-\frac{pv}{r}+\frac{j_z^2}{\sigma}+\frac{1}{r}\frac{\partial}{\partial r}\left(r\kappa\frac{\partial T}{\partial r}\right), \quad (2c)$$

$$\frac{\partial B_\varphi}{\partial t}=\frac{\partial}{\partial r}\left[\frac{1}{\mu_0\sigma r}\frac{\partial}{\partial r}\left(rB_\varphi\right)\right], \quad (2d)$$

$$j_z=\frac{1}{\mu_0 r}\frac{\partial(rB_\varphi)}{\partial r}. \quad (2e)$$

Here ρ, v, and u are the mass density, velocity of expansion, and specific internal energy, respectively. j_z is the axial current density, E_z is the axial electric field, where $j_z=\sigma E_z$, and B_φ is the azimuthal magnetic field, and μ_0 is the magnetic permeability. The temperature of the wire, $T(\rho,u)$ is taken to be a function of density and internal energy, as determined by the SESAME database [29]. $p(\rho,T)$ and $\sigma(\rho,T)$ are the material pressure and electrical conductivity, both as a function of temperature and density. The internal pressure of the material is determined from interpolations of the SESAME data [29]. Due to the time scales of interest, very little thermal conduction is observed, and it is sufficient to roughly approximate the thermal conductivity $\kappa(\rho T)$ by the Wiedemann-Franz law [30]. Note that such treatment of the thermal conductivity assumes that the predominant thermal conduction mechanism is through degenerate transport processes. In similar MHD experiments, it was indicated that the EOS of the background gas can be roughly approximated, without jeopardizing the accuracy of the simulation [13]. For these simulations, the EOS of the background gas is determined using ideal gas approximations, and the electrical conductivity is assumed to be zero. It was found that a better fit between experiments and MHD simulations was achieved by decreasing the simulated wire length by ~10%. It is suspected that this is the result of plasma formation at the contact electrodes, thus shunting any EW behavior in these regions, similar to what is observed in Refs. [31,32].

Equations (2a)–(2c) define the dynamics of the EW, from which the temperature and density can be derived. With these parameters, the remaining material properties can be determined. Equation (2d) defines the diffusion of the magnetic field into the EW. Note that the given equation neglects the effects of the EW expanding into the magnetic field. This is a reasonable assumption given that very little expansion of the EW is experienced on the initial time scales during which the magnetic field exhibits a steep radial gradient. Knoepfel indicates that the magnetic diffusion time can be approximated by $\tau_d \approx r^2\mu_0\sigma \approx 320$ ns [33]. The simulated magnetic diffusion time is generally on the order of 100–200 ns. This slightly shorter time scale is the result of Joule heating of the EW, thus allowing for more rapid diffusion of the magnetic field. For the time scales of interest here, magnetic diffusion plays a fairly insignificant role. Nonetheless, magnetic diffusion is accounted for in the simulation.

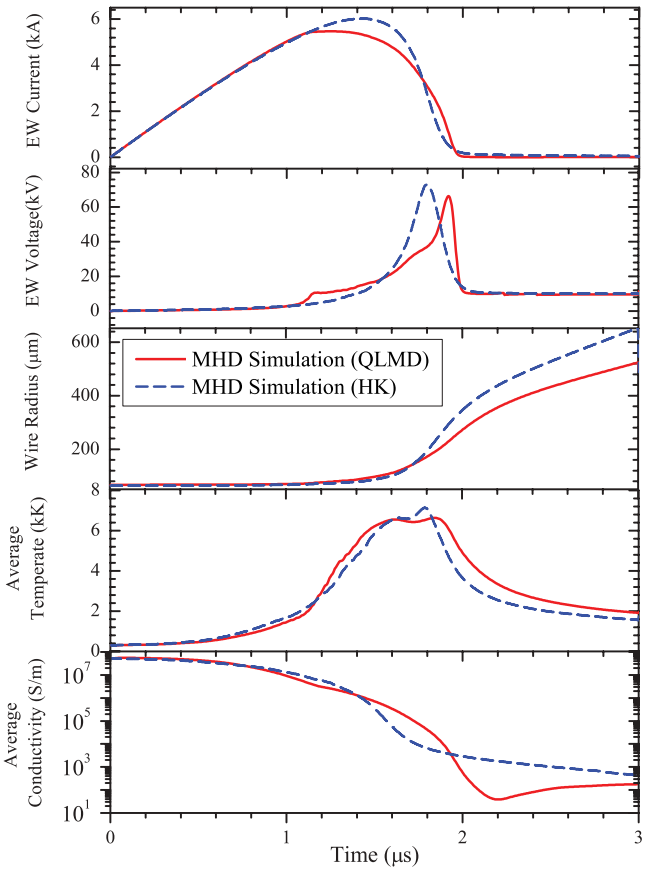

FIG. 2. (Color online) MHD simulated waveforms. $V_0 = 15$ kV, and the copper wire is 18 cm in length with a 127-μm diameter. MHD simulation with QLMD data is shown by the solid red line, and MHD simulation with HK data is shown by the dashed blue line.

Equations (2a)–(2e) are solved explicitly using multipoint finite difference techniques [34] with a Lagrangian coordinate system [28,33]. The MHD equations are solved simultaneously with the constraining circuit equations to derive the voltage and current waveforms, along with the physical parameters of the EW throughout the dense plasma formation (cf. Fig. 2).

Two different conductivity models are applied for both silver and copper. For silver, conductivity from the Lee-More-Desjarlais (LMD) [35,36] algorithm is applied. Copper uses the quantum LMD (QLMD) data, which involves fitting the LMD algorithm to the quantum molecular dynamics (QMD) simulation methods of Ref. [37]. The LMD and QLMD data have been verified to be very accurate in high temperature EW experiments; however, very little testing has been conducted in the sub-eV regime. The second conductivity model applied is

based on the empirical equation given by Knoepfel (HK) [33]:

$$\sigma_{HK}(\rho,T) = \frac{\sigma_0}{1+\beta(T-T_0)}\left(\frac{\rho}{\rho_0}\right)^{\alpha} \tag{3}$$

Here T_0 is the room temperature, 298 K, ρ_0 is the mass density at room temperature, and σ_0 is the electrical conductivity at room temperature. The parameters α and β are the mass density and temperature coefficients. Experiments and comparison with the LMD and the QLMD data indicate $\alpha = 2.4$ and $\beta = 0.002$ for copper and $\alpha = 2.6$ and $\beta = 0.009$ for silver provide the best performance from the HK conductivity. Note that the values given here deviate slightly from those presented by Knoepfel [33]. It is suspected that this is due to the fact that the values given here are specifically optimized to our limited temperature-density range, whereas Knoepfel's values are intended to cover a wider range than is discussed here.

As the LMD and QLMD conductivities are based on inherently more complex models, they have a significantly wider range of validity. Alternatively, a consequence of the HK conductivity's simplicity is the limited parameter range for which it is accurate. The focus of this paper is to confirm the LMD and QLMD conductivity in the sub-eV regime and similarly explore the validity of the HK conductivity.

It was shown by Lindemuth *et al.* that if the exploding conductor expansion is not sufficiently limited, the rapidly growing cross section will ultimately result in decreases in resistance [27]. However, with the HK conductivity, the resistance begins to diverge to infinity at lower density. It is therefore concluded that the HK equation fails at lower density (significant error below 1 gm/cm^3) and is incapable of properly modeling cross-sectional growth induced resistance decreases in EW experiments. Additionally, it is known that for certain conditions, the plasma conductivity will increase with increasing temperature [36–39], yet another phenomenon not captured by the HK conductivity.

The results of a MHD simulation for typical EW parameters are given in Fig. 2 for both QLMD conductivity and HK conductivity. The "average conductivity" in Fig. 2 was calculated using $\sigma_{\mathrm{Av}}(t) = I(t)Z_0/[V_{\mathrm{R}}(t)A_{\mathrm{w}}(t)]$, where Z_0 is the wire length and $A_{\mathrm{w}}(t)$ is the time-dependent wire cross-sectional area. As shown, the QLMD and HK conductivity models demonstrate the same approximate behavior. The current initially follows an underdamped RLC type discharge. During this time, the conductivity of the wire is still very high, and Joule heating is minimized, as is demonstrated by the lower temperature for times less than 1 μs. As the temperature of the wire increases, conductivity decreases, and the rate of Joule energy deposition rapidly increases, thus quickly driving the temperature beyond 6 kK. Note that the vaporization temperature of copper is approximately 2843 K [40], and the critical temperature is approximately 8390 K [39]. This increase in temperature also corresponds to rapid expansion of the EW plasma column. This sharp launch to higher temperature and lower density results in a substantial decrease in electrical conductivity. As a result, the resistance of the EW increases to several orders of magnitude times its initial value. The corresponding increase in EW resistance forces a sharp interruption in EW current and large EW voltage, corresponding to the induced di/dt. At later times, once the current is completely interrupted, i.e., $di/dt \sim 0$, the voltage across the EW [cf. V_R in Eq. (1)] drops sharply. At this time, the current is also sufficiently low that the capacitor is only slowly losing charge through current flow, and the voltage across the EW becomes approximately constant. Figure 2 also demonstrates that by exploding the wires in air at atmospheric pressure, expansive cooling of the EW is critical to the fundamentals of the experiments shown here, as is demonstrated by the decaying EW temperature after 2 μs.

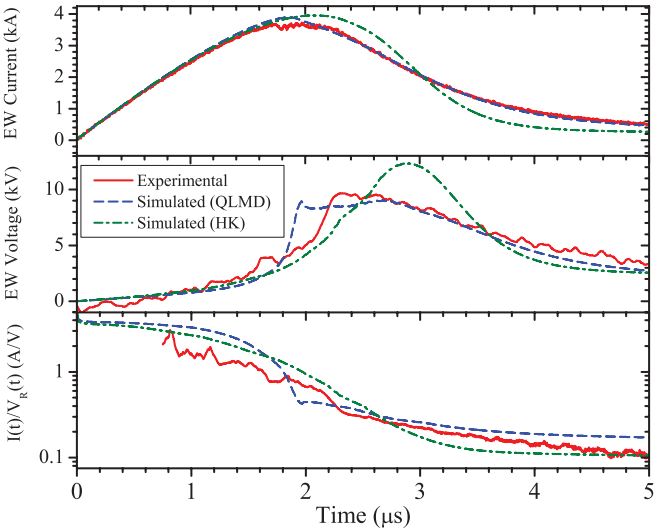

FIG. 3. (Color online) Experimental and simulated voltage and current waveforms. $V_0 = 7.5$ kV, and the copper wire is 18 cm in length with a 127-μm diameter. Experiment is shown by the solid red line, MHD simulation with QLMD data is shown by the dashed blue line, and MHD simulation with HK data is shown by the dash-dotted green line.

IV. RESULTS

Experimental and simulated voltage and current waveforms, as well as the current to voltage ratio for copper wire, with an initial capacitor voltage of 7.5 kV are depicted in Fig. 3. For an initial voltage of 7.5 kV, it is observed that the current excitation provided by the system is insufficient to drive the EW through the steep resistive transition. As shown in Fig. 3, MHD simulation with the QLMD conductivity is able to accurately capture the behavior of the EW. Similarly, MHD simulation with the HK conductivity is able to come close to the experimentally observed behavior but to a lower degree of accuracy than the QLMD data. Comparison of the I-V ratio correlates to a comparison of the time evolution of the electrical conductivity, given that the wire radius from the MHD simulations and experiment all roughly agree with one another. As is shown in Fig. 3, the same general behavior of the I-V ratio for both MHD simulations and experiments indicates that the electrical conductivity is reasonably represented by either model.

Figure 4 depicts an additional experiment with a copper EW and a charging voltage of 20 kV. With this excitation, the EW undergoes the rapid resistance increase similar to what would be observed in an EW based opening switch. MHD simulations with the QLMD conductivity are able to predict this behavior reasonably well; however, the time of current interruption is slightly underestimated. With the HK conductivity, the

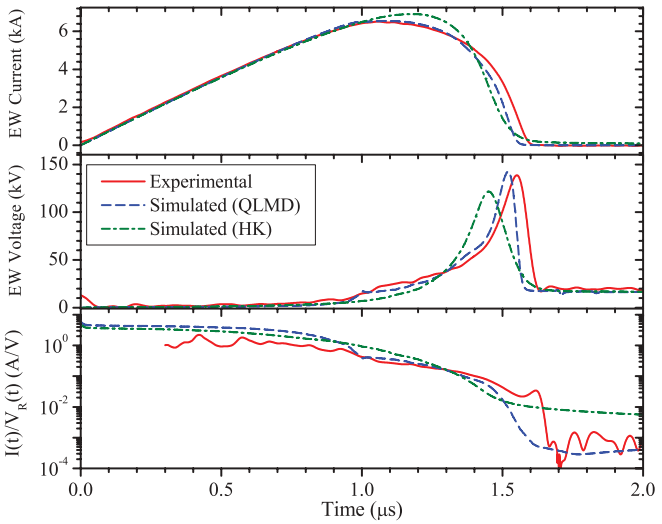

FIG. 4. (Color online) Same as Fig. 3, with $V_0 = 20$ kV.

peak current is overpredicted, and again, the interruption time is underestimated. Nonetheless, the overall dynamics of the explosion are captured with the HK conductivity, despite the simplicity of the model. The I-V ratio given in Fig. 4 indicate that, although the time at which the conductivity transition occurs is slightly underestimated, the MHD simulation with the QLMD conductivity accurately captures the conductivity evolution experimentally observed. Simulations with the HK data indicate that the conductivity is overestimated by as much as an order of magnitude in the late stages of the experiment. Regardless, as stated, the voltage and current waveforms are fairly well replicated when applying the HK conductivity.

Similar observations have been made with experimentation and simulation of silver EWs. Figure 5 shows the voltage and current waveforms for an initial voltage of 15 kV. Again, Joule heating of the EW drives the material to the point where a sharp drop in current is experienced. As expected the LMD based MHD simulation is able to closely follow the experimental

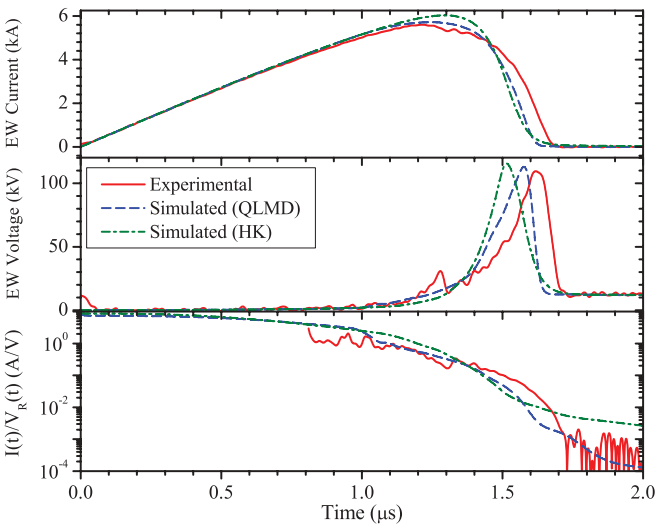

FIG. 5. (Color online) Same as Fig. 3, with silver wire, LMD model, $V_0 = 15$ kV.

data. Similarly, the HK based MHD simulation is also able to follow the experimental data, to a reasonable degree. Again, in evaluating the I-V ratio it is observed that the LMD based MHD simulations capture the experimentally observed conductivity evolution. However, again, the HK based MHD simulation overpredicts the conductivity by roughly an order of magnitude.

It should be noted that the overall quantitative error in the calculations is presently undetermined, primarily due to the various potential limitations of the techniques presented here. Nevertheless, some study of uncertainty in wire parameters exists in the open literature (refer to Drake *et al.* [41]): Using MHD and statistical variation of wire radius, length, and resistance, the effects of uncertainty in the wire parameters on the resulting simulated voltage and current waveforms, compared to experimental data, are comprehensively discussed. It is possible that similar uncertainty in the wire parameters for the experiments discussed here contributes to the error in these MHD simulations. Additionally, the application of the arbitrary phase, temperature-density controlled model also has limitations. Applying such models, especially in the two phase liquid-vapor region below the critical point, has been questioned before.

V. CONCLUSION

Ultimately, several experiments were run at charging voltages of $V_0 = 7.5$, 10, 15, and 20 kV for both copper and silver. In all cases, the LMD and QLMD based MHD simulations demonstrated approximately the same level of accuracy summarized in Figs. 3–5. In general, the accuracy of the methodology described here is strongly dependent upon the accuracy of the SESAME data, validity of the one-dimensional treatment of the EW, and numerical techniques applied. Regardless, given the reasonable fit between experimental and simulated waveforms, it is concluded that the LMD and QLMD data are suitable for modeling in the sub-eV regime.

Expectedly, the HK dependent MHD simulations demonstrated a few issues. In general, the HK conductivity gives higher conductivity than experimentally observed data, prior to the current interruption process (i.e., lower predicted EW voltages and higher currents are simulated prior to current interruption). Additionally, simulations with the HK conductivity have a tendency to predict current interruption where such behavior is not experimentally observed. However, when current interruption is observed, the HK dependent MHD predicts much less aggressive current interruption in the final stages of the interruption process. However, implementation of an analytical approximation is appealing, given its accessibility and significant decrease in necessary computing power as compared to interpolations of large data sets. For example, in these studies, the MHD simulations using the HK data were completed in less than a minute on a 32 core server workstation, roughly one-tenth of the time needed for the LMD and QLMD MHD simulations. It is possible that the inaccuracies may be considered acceptable in first-order approximations, for instance, for quick calculation of fuse opening switch performance in the early design stages of a pulsed power system, again, given the simplicity and low computational demand associated with the HK data.

ACKNOWLEDGMENTS

The authors would like to thank Sandia National Laboratories, which has, in part, supported this research through a fellowship from the National Physical Sciences Consortium. Dr. Desjarlais and Dr. Cochrane of Sandia National Laboratories are thanked for providing the LMD and QLMD data and useful discussions. Los Alamos National Laboratory is thanked for supplying the SESAME equation of state database.

[1] A. W. DeSilva and H.-J. Kunze, Phys. Rev. E **49**, 4448 (1994).
[2] A. W. DeSilva and J. D. Katsouros, Phys. Rev. E **57**, 5945 (1998).
[3] I. Krisch and H.-J. Kunze, Phys. Rev. E **58**, 6557 (1998).
[4] J. F. Benage, W. R. Shanahan, and M. S. Murillo, Phys. Rev. Lett. **83**, 2953 (1999).
[5] V. N. Korobenko, A. D. Rakhel, A. I. Savvatimiski, and V. E. Fortov, Phys. Rev. B **71**, 014208 (2005); **71**, 099902(E) (2005).
[6] V. N. Korobenko and A. D. Rakhel, Phys. Rev. B **75**, 064208 (2007).
[7] J. Clérouin, P. Noiret, P. Blottiau, V. Recoules, B. Siberchicot, P. Renaudin, C. Blancard, G. Faussurier, B. Holst, and C. E. Starrett, Phys. Plasmas **19**, 082702 (2012).
[8] D. Sheftman, D. Shafer, S. Efimov, and Ya. E. Krasik, Phys. Plasmas **19**, 034501 (2012).
[9] A. Grinenko, V. T. Gurovich, A. Saypin, S. Efimov, Y. E. Krasik, and V. I. Oreshkin, Phys. Rev. E **72**, 066401 (2005).
[10] V. I. Oreshkin, R. B. Baksht, A. Yu. Labetsky, A. G. Rousskikh, A. V. Shishlov, P. R. Levashov, K. V. Khishchenko, and I. V. Glazyrin, Tech. Phys. **49**, 843 (2004).
[11] D. Sheftman and Ya. Krasik, Phys. Plasmas **17**, 112702 (2012).
[12] D. Sheftman and Ya. E. Krasik, Phys. Plasmas **18**, 092704 (2011).
[13] A. E. Barysevich and S. L. Cherkas, Phys. Plasmas **18**, 052703 (2011).
[14] J. Stephens, A. Neuber, and M. Kristiansen, Phys. Plasmas **19**, 032702 (2012).
[15] J. Stephens and A. Neuber, Phys. Plasmas **19**, 060702 (2012).
[16] J. Stephens, W. Mischke, and A. Neuber, *IEEE Transactions on Plasma Science*, Vol. 40 (IEEE, New York, 2012), pp. 2517–2522.
[17] M. A. Elsayed, A. A. Neuber, J. C. Dickens, J. W. Walter, M. Kristiansen, and L. Altigilbers, Rev. Sci. Instrum. **83**, 024705 (2012).
[18] B. M. Novac, I. R. Smith, P. Senior, M. Parker, and G. Louverdis, Rev. Sci. Instrum. **81**, 054706 (2010).
[19] G. A. Mesyats, *Pulsed Power* (Springer, Berlin, 2004).
[20] D. R. McCauley, D. W. Belt, J. J. Mankowski, J. C. Dickens, A. A. Neuber, and M. Kristiansen, IEEE Trans. Plasma Sci. **36**, 2691 (2008).
[21] K. B. Abramova, N. A. Zlatin, and B. P. Peregud, Sov. Phys. JETP **42**, 1019 (1976).
[22] A. G. Rousskikh, V. I. Oreshkin, S. A. Chaikovsky, N. A. Labetskaya, A. V. Shishlov, I. I. Beillis, and R. B. Baksht, Phys. Plasmas **15**, 102706 (2008).
[23] G. S. Sarkisov, S. E. Rosenthal, K. R. Cochrane, K. W. Struve, C. Deeney, and D. H. McDaniel, Phys. Rev. E **71**, 046404 (2005).
[24] S. I. Tkachenko, K. V. Khishchenko, V. S. Vorob'ev, P. R. Levashov, I. V. Lomonosov, and V. E. Fortov, High Temp. **39**, 674 (2001).
[25] K. V. Khishchenko, S. I. Tkachenko, P. R. Levashov, I. V. Lomonosov, and V. S. Vorob'ev, Int. J. Thermophys. **23**, 1359 (2002).
[26] D. Bakulin, V. F. Kuropatenko, and A. V. Luchinskii, Sov. Phys. Tech. Phys. **21**, 1144 (1976).
[27] I. R. Lindemuth, J. H. Brownell, A. E. greene, G. H. Nickel, T. A. Oliphant, and D. L. Weiss, J. Appl. Phys. **57**, 4447 (1985).
[28] D. Schnack, *Lectures in Magnetohydrodynamics: With an Appendix on Extended MHD* (Springer, Heidelberg, 2009).
[29] Los Alamos National Laboratory, Report No. LA-UR-92-3407, edited by S. P. Lyon and J. D. Johnson, 1992 (unpublished).
[30] G. Wiedemann and R. Franz, Ann. Phys. **89**, 497 (1853).
[31] S. A. Pikuz, T. A. Shelkovenko, D. B. Sinars, J. B. Greenly, Y. S. Dimant, and D. A. Hammer, Phys. Rev. Lett. **83**, 4313 (1999).
[32] D. B. Sinars, T. A. Shelkovenko, S. A. Pikuz, M. Hu, V. M. Romanova, K. M. Chandler, J. B. Greenly, D. A. Hammer, and B. R. Kusse, Phys. Plasmas **7**, 429 (2000).
[33] H. Knoepfel, *Magnetic Fields: A Comprehensive Theoretical Treatise for Practical Use* (Wiley, New York, 2000).
[34] J. Li and Y. Chen, *Computational Partial Differential Equations Using* MATLAB (Taylor and Francis, Boca Raton, FL, 2008).
[35] Y. T. Lee and R. M. More, Phys. Fluids **27**, 1273 (1984).
[36] M. P. Desjarlais, Contrib. Plasma Phys. **41**, 267 (2001).
[37] M. P. Desjarlais, J. D. Kress, and L. A. Collins, Phys. Rev. E **66**, 025401 (2002).
[38] S. Kuhlbrodt and R. Redmer, Phys. Rev. E **62**, 7191 (2000).
[39] V. E. Fortov and I. T. Iakubov, *The Physics of Non-ideal Plasma* (World Scientific, Singapore, 2000).
[40] *Explosively Driven Pulsed Power*, edited by A. A. Neuber (Springer, Berlin, 2005).
[41] R. R. Drake, D. R. Koenig, and J. H. J. Niederhaus https://cfwebprod.sandia.gov/cfdocs/CCIM/docs/ExplodingWireUUR_paper.pdf.